Chinese Journal of
POLYMER SCIENCE

RESEARCH ARTICLE

https://doi.org/10.1007/s10118-025-3474-8
Chinese J. Polym. Sci. **2026**, *44*, 189–197

Influence of Soft Segment Length on the Dielectric Polarization Behavior of Ketal-containing Polyurethane Elastomer

Xue Mei[a], Wan Lu[a], Jian-Rong Dong[a], Ke-Heng Pan[a], Jun-Jie Tan[a], Hong-Ye Yan[a], Jun Wu[b], Yu Zhou[a], and Hong-Xiang Chen[a,c*]

[a] *School of Chemistry and Chemical Engineering, Wuhan University of Science and Technology, Wuhan 430081, China*
[b] *State Key Laboratory of Advanced Refractories, Wuhan University of Science and Technology, Wuhan 430081, China*
[c] *Hubei Key Laboratory of Pollutant Analysis & Reuse Technology, Hubei Normal University, Huangshi 435002, China*

Electronic Supplementary Information

Abstract Polyurethane elastomers exhibit high dielectric constants owing to their polar groups, and can be used as energy storage capacitors. Energy storage depends not only on the dielectric constant but also on the dielectric loss. However, the relationship between chain structure and dielectric properties is not yet clear. Ketal-containing crosslinked polyurethane elastomers were prepared using cyclic ketal diol as a chain extender. The effect of the soft segment length on the dielectric properties and energy storage was investigated. The cause of the change in the dipolar polarization with the soft segment length was analyzed. As the soft segment length increased, the hard-soft hydrogen bonding decreased, whereas the hard-hard hydrogen bonding increased. Under the action of an electric field, the polar bonds in the ketal-containing polyurethane elastomer overcome the hydrogen bonding between hard-soft segments to produce polarization; meanwhile, they also experience crankshaft motions to generate polarization. The former has a relatively high relaxation activation energy of approximately 10–20 kJ·mol^{-1}, resulting in a large dielectric loss. The latter has a relatively low relaxation activation energy, approximately 0.7–1.7 kJ·mol^{-1}, leading to low dielectric loss. As a result, the dielectric constant showed a decreasing trend, and the dielectric loss gradually decreased. This study provides a theoretical foundation for improving the dielectric properties of polyurethane elastomers.

Keywords Dielectric polarization; Polyurethane elastomer; Soft segment length; Intermolecular interaction

Citation: Mei, X.; Lu, W.; Dong, J. R.; Pan, K. H.; Tan, J. J.; Yan, H. Y.; Wu, J.; Zhou, Y.; Chen, H. X. Influence of soft segment length on the dielectric polarization behavior of ketal-containing polyurethane elastomer. *Chinese J. Polym. Sci.* **2026**, *44*, 189–197.

INTRODUCTION

Polymer dielectrics have a charge storage capacity owing to their polarization under the influence of an electric field. Typical polymer dielectrics, such as poly(vinylidene fluoride) (PVDF),[1–3] biaxially oriented polypropylene (BOPP),[4] polycarbonate (PC),[5] and polyimide (PI),[6,7] can be used as energy storage materials for film capacitors. Therefore, they have received widespread attention.[8–11] The energy storage density depends on the dielectric constant of the polymer and the intensity of the applied electric field, whereas the energy storage efficiency is mainly restricted to the magnitude of the dielectric loss.[12,13] The dielectric constant of a polymer mainly depends on the dipolar polarization, whereas the dielectric loss mainly stems from the energy loss in the dipolar relaxation process.[14,15] However, the correlative relationship between the polarization relaxation behavior of dipoles and the chain structure of the polymer requires further study.

The growth of the alkyl side-chain length disrupted the close packing among chains in the fluorene-benzocyclobutene-based polymer, thus leading to a slight decrease in the dielectric constant and a simultaneous decreasing trend in the dielectric loss.[16] Dynamic covalent cross-linking of polyethylene was formed by the reaction of maleic anhydride grafted with epoxy resin. The dielectric constant was higher than that of linear polyethylene and the dielectric loss remained below 0.02.[17] Films obtained by blending PVDF with a poly(vinylidene fluoride-trifluoroethylene-chlorofluoroethylene) terpolymer exhibited a high dielectric constant and low polar dielectric loss.[18] It can be seen from the above literature that the dielectric polarization of polymer dielectrics mainly relies on the type and content of polar groups, whereas the dipolar relaxation is influenced by the interaction between polymer chains.

Polyurethane has a phase-separated cross-linked structure and shows excellent mechanical properties compared with the above-mentioned dielectrics.[19] Meanwhile, the polar N—H, C—O, and C=O groups can provide a relatively high dielectric constant for polyurethane.[20–22] The ketal-containing polyurethane dielectric elastomer showed a dielectric

* Corresponding author, E-mail: chenhongxiang@wust.edu.cn
Received August 19, 2025; Accepted October 8, 2025; Published online December 22, 2025

constant of 11.9 and a dielectric loss of 0.045 at 10^3 Hz in our previous study, but its dielectric loss was relatively high.[23] The dielectric constant and energy storage density of polyurethane can be improved by blending it with polyamide (PA)[24] or PVDF.[25] In addition, amorphous poly(hydroxy urethane) prepared by the reaction of diamine and cyclic carbonate exhibited a dielectric constant of 8.4, dielectric loss of 0.03, and breakdown strength of 428 MV·m^{-1}.[26] It can be seen that the dielectric polarization of polyurethane is related to the type and content of polar groups. However, the impact of the interaction between the chain segments on the polarization relaxation behavior of dipoles remains unclear. Therefore, if the interaction between chain segments can be regulated in polyurethane, its effect on the dielectric polarization behavior can be unveiled. This is of great significance for improving the energy storage density and efficiency of polyurethane elastomers.

Dynamic ketal-containing polyurethane was chosen to study the intermolecular interactions between chains. When the soft segment content remained relatively constant, the soft segment length was changed to modify the interactions between the molecular chains. Simultaneously, the dynamic exchange of the ketal endowed polyurethane with thermal healing performance. Polyurethane elastomers were prepared using poly[(oxytetramethylene) glycols] (PTMG) with different molecular weights as soft segments, diphenylmethane diisocyanate (MDI) and ketal diol as hard segments, and glycerol as the cross-linking agent. The influence of soft segment length on the dielectric constant, dielectric loss, energy storage density, and energy storage efficiency of polyurethane was studied. In addition, the effects of the soft segment length on the dielectric polarization behavior were analyzed by intermolecular hydrogen-bonding interaction, phase separation structure and relaxation activation energy. This work can provide a feasible way for improving the dielectric properties of polyurethane.

EXPERIMENTAL

Materials

Poly[(oxytetramethylene) glycols] (M_n=650, PTMG650; M_n=1000, PTMG1000; M_n=2000, PTMG2000; M_n=3000, PTMG3000) were obtained from Korea PTG Co., Ltd. 4,4′-Diphenylmethane diisocyanate (MDI) was purchased from Kumho Mitsui Chemicals Inc. *N*,*N*-dimethylacetamide (DMAc) and ethanol were purchased from Sinopharm Chemical Reagent Co., Ltd. 1,4-Cyclohexanedione (CHD) was obtained from Shanghai Macklin Biochemical Technology Co., Ltd. Glycerol was purchased from Tianjin Tianli Chemical Reagent Co., Ltd. Anhydrous sodium sulfate was purchased from Tianjin Xinfa Chemical Reagent Co., Ltd. The A-15 catalyst was purchased from Jiangyin Chemical Reagent Factory Co., Ltd. The A-15 catalyst and sodium sulfate were used after activation at 120 and 150 °C for 2 h, respectively. DMAc was purified *via* vacuum distillation.

Synthesis of Cyclohexanedione Glycerol Ketal

1,4-Cyclohexanedione glycerol ketal (CHDGK) was synthesized based on our previous study.[23] Glycerol (4.97 g, 54 mmol), and 1,4-cyclohexanedione (3.03 g, 27 mmol) were added to a reaction flask. The A-15 catalyst (1 wt% glycerol) and water-carrying agent Na_2SO_4 (25 wt% reactant) were added to the reaction mixture and stirred at 100 °C for 10 h. After filtration, 1,4-cyclohexadione glycerol ketal containing a minute quantity of glycerol was obtained. A schematic diagram of the reaction is shown in Fig. 1(a) and the ^{1}H-NMR spectrum of the product is shown in Fig. 1(b).

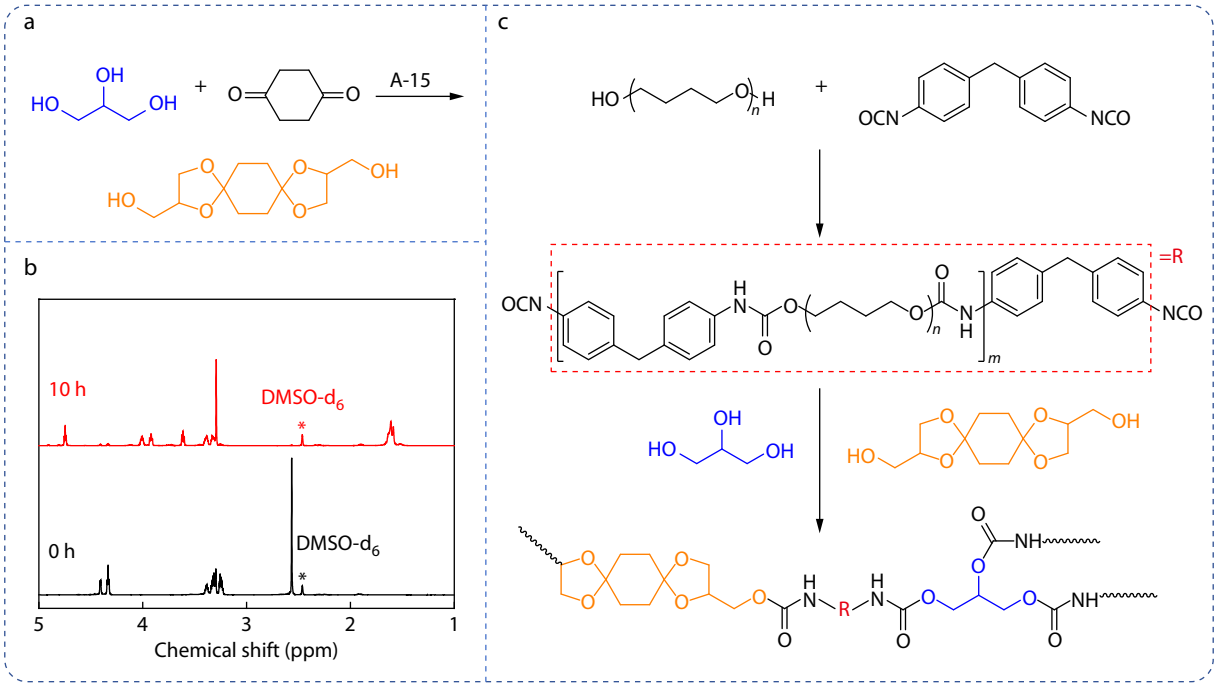

Fig. 1 Cyclohexadione-glycerol ketal: (a) schematic diagram of synthesis and (b) ^{1}H-NMR spectra; (c) Schematic diagram of preparation for ketal-containing cross-linked polyurethane elastomers.

https://doi.org/10.1007/s10118-025-3474-8

Preparation of Ketal-containing Polyurethane Elastomers

PTMG650 was placed in a four-necked flask and dehydrated at 120 °C for 2 h. After MDI was added dropwise to the flask, the mixture was stirred under N_2 at 60 °C for 2 h to form a polyurethane prepolymer. The chain extender and the crosslinking agent with a CHDGK/glycerol molar ratio of 4/3 were added to the flask. An appropriate amount of DMAc was added to adjust the viscosity. The reaction mixture was stirred uniformly and poured into a mold. After demolding, the sample was cured at 100 °C for 10 h to form the ketal-containing cross-linked polyurethane (**PUCK-C*x***). A schematic diagram of the preparation process is shown in Fig. 1(c). At a constant soft-segment content (64 wt%), cross-linked polyurethane samples with different soft-segment lengths were obtained by varying the molecular weight of PTMG. The designations, compositions, and swelling degrees of the samples are listed in Table 1.

Characterization

The ^{1}H-NMR spectrum of CHDGK was recorded on an Agilent 600 MHz DD2 spectrometer (Agilent) in DMSO-d_6, using tetramethylsilane as an internal standard. The FTIR spectra of **PUCK-C*x*** were obtained in the attenuated total reflection mode using a Vertex 70 Fourier transform infrared spectrometer (Bruker) in the range of 4000–600 cm^{-1} at a resolution of 4 cm^{-1}. The thermal behavior of **PUCK-C*x*** was investigated using a DSC 4000 differential scanning calorimeter (PerkinElmer) in the temperature range from −90 °C to 200 °C under N_2 atmosphere at a heating rate of 10 °C·min^{-1}. The **PUCK-*x*** samples were soaked in acetone for 30 days. The swelling degree was calculated as $Q = (m_1/\rho_1 + m_2/\rho_2)/(m_2/\rho_2)$, where m_1 and m_2 are the weights of the solvent and original polymer, respectively, and ρ_1 and ρ_2 are the densities of the solvent and original polymer, respectively. AFM images of **PUCK-C*x*** samples were collected using a Dimension ICON atomic force microscope (Bruker) in tapping mode at a scanning frequency of 1 Hz with a nominal spring constant of 0.4 N·m^{-1}. The thermal stability of **PUCK-C*x*** was determined using an STA 2500 integrated thermal analyzer (Netzsch) under N_2 atmosphere from room temperature to 600 °C at a heating rate of 10 °C·min^{-1}. Tensile testing of **PUCK-C*x*** at room temperature was performed using a UTM 6503 electronic universal testing machine (SUNS) at 50 mm·min^{-1} cross-head speed. The dimensions of the dumbbell-shaped specimen of type II were 75 mm × 4 mm × 2 mm according to the ISO 37—2005 and the average value was obtained from the results of three tests. The specimen was cut off with a blade, immediately combined, slightly pressed, and healed at 100 °C for 5 h. The healing efficiency was obtained using the equation E_h (%) = $\sigma_{healed}/\sigma_{original}$ × 100%, where σ_{healed} and $\sigma_{original}$ represent the tensile strengths of the healed and original specimens, respectively.

The dielectric properties of **PUCK-C*x*** samples coated with silver pulp were measured using a HIOKI 3532-50 LCR dielectric impedance analyzer (HIOKI) under a voltage of 5 V from 10^2 Hz to 10^5 Hz at different temperatures. The dielectric constant (ε') was calculated using Eq. (1):

$$\varepsilon' = \frac{C \cdot d}{\varepsilon_0 \cdot A} \quad (1)$$

where C is the electrostatic capacitance of the equivalent circuit model, d is the thickness of the sample, ε_0 is the vacuum permittivity (8.85×10^{-12} F·m^{-1}), and A is the area of the capacitor plate. The *P-E* loops were characterized using a Polyk testing system equipped with a 10 kV Trek high-voltage source at 100 Hz. The discharged energy density U_E and energy storage efficiency η were calculated using Eqs. (2) and (3), respectively:[27–29]

$$U_E = \int_{P_r}^{P_m} E \mathrm{d}P \quad (2)$$

$$\eta = \frac{U_E}{U_E + U_L} \quad (3)$$

where E, P, P_r, P_m, and U_L are electric field intensity, polarization, remnant polarization, the maximum polarization, loss energy density, respectively.

RESULTS AND DISCUSSION

Preparation, Mechanical Properties, and Thermal Properties of the Ketal-containing Polyurethane Elastomers

Ketals with two hydroxyl groups can be synthesized from glycerol and 1,4-cyclohexanedione. The ^{1}H-NMR spectrum of the product is shown in Fig. 1(b) and Fig. S1 (in the electronic supplementary information, ESI). It can be observed that the peak at 2.57 ppm is assigned to —CH_2— proton of 1,4-cyclohexanedione, and the peaks at 3.38, 3.31, 3.25 ppm are assigned to —CH< and —CH_2— protons of glycerol, respectively. After 10 h of reaction, the peak at 2.57 ppm nearly disappeared, while a new peak assigned to the —CH_2— protons of the six-membered carbon ring in the cyclic ketal appeared at 1.62 ppm. It can be inferred that glycerol reacts with 1,4-cyclohexanedione to form a ketal containing two hydroxyl groups. Moreover, the conversion rate was calculated according to the area of the two peaks up to 99%.

PUCK-C*x* samples were obtained by chain extension of CHDGK and varying the length of the soft segment. The infrared spectra of the samples are shown in Fig. 2. The bands attributed to the carbamate N—H stretching vibration and bending vibration appeared at 3294 and 1534 cm^{-1}, respectively. The bands at 1731 and 1710 cm^{-1} correspond to free and hydrogen-bonded carbamate C=O stretching vibrations, respectively. The band at 1103 cm^{-1} was assigned to the C—O stretching vibration of polyether. The absorption band at 1260 cm^{-1} is attributed to the asymmetric stretching vibration of O—C—O in the five-membered cyclic ketal.[23] Moreover, the NCO and OH absorption bands completely disappeared from the spectra. This indicated that the isocyanate groups in MDI completely reacted with the hydroxyl groups

Table 1 Designation, feed molar ratio, and swelling degree of ketal-containing cross-linked polyurethane elastomers.

Sample	Composition (molar ratio)	Swelling degree
PUCK-C1	MDI/PTMG650/CHDGK/glycerol (21.51/17.88/1.69/1.27)	2.18
PUCK-C2	MDI/PTMG1000/CHDGK/glycerol (29.15/17.88/5.27/3.96)	2.22
PUCK-C3	MDI/PTMG2000/CHDGK/glycerol (53.17/17.88/16.54/12.41)	2.41
PUCK-C4	MDI/PTMG3000/CHDGK/glycerol (76.16/17.88/27.35/20.52)	2.63

https://doi.org/10.1007/s10118-025-3474-8

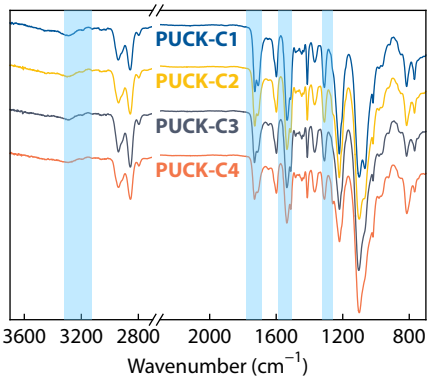

Fig. 2 FTIR spectra of ketal-containing cross-linking polyurethane elastomers.

in PTMG, glycerol, and CHDGK to form carbamate groups. In addition, none of the samples dissolved in acetone, but only swelled, as shown in Table 1 and Fig. S2 (in ESI). It can be concluded that all **PUCK-C*x*** samples formed a cross-linked structure. Moreover, the cross-linking degree decreased with an increase in soft segment length.

The stress-strain curves of the ketal-containing cross-linked polyurethane samples are shown in Fig. S3 (in ESI), and the tensile strength, elongation at break, toughness, and Young's modulus are listed in Table S1 (in ESI). It can be observed that all samples exhibited the tensile behavior of the elastomer. The tensile strength of the sample continued to increase with an increase in the soft segment length, and the elongation at break showed an increasing trend. It can be inferred that the difference in soft segment length can cause changes in the chain structure and intermolecular interactions in the elastomer. In addition, all **PUCK-C*x*** samples exhibited initial thermal decomposition temperatures above 280 °C (Fig. S4 in ESI), indicating good thermal stability. **PUCK-C*x*** samples also displayed thermal healing ability (Fig. S5 in ESI).

These results demonstrated that ketal-containing cross-linked polyurethane elastomers with different soft segment lengths were obtained using CHDGK as a chain extender and glycerol as a cross-linking agent.

Influence of Soft Segment Length on the Phase Structure and Intermolecular Interaction

DSC, AFM, and FTIR analysis were used to probe the influence of soft segment length on the interchain interaction in polyurethane.

DSC curves of **PUCK-C*x*** samples are shown in Fig. 3. In the low-temperature region, the glass transition of the soft segments occurred in all samples, and the glass transition temperature (T_g) decreased with an increase in the soft segment length. In the high-temperature region, no obvious melting phenomenon occurred, but an endothermic phenomenon existed within a wide temperature range. In **PUCK-C*x***, PTMG comprises the soft segment, whereas the MDI and CHDGK units comprise the hard segment. The intermolecular interaction between the soft segments is mainly due to van der Waals forces. Thus, PTMG has good flexibility, and the glass transition of soft segments occurs in the low-temperature region. The hard segments have a relatively high content of polar bonds, and the intermolecular interactions between the hard segments are relatively strong. This can bring about the thermodynamic incompatibility of the hard and soft segments, leading to phase separation phenomena in all the samples. However, glycerol, as a cross-linking point, can hinder the crystallization of hard segments and restrict the crystallization of soft segments. Therefore, no obvious melting phenomenon was observed. It can be found from the above analyses that the interchain interaction plays a key role in the phase structure of ketal-containing polyurethane.

Hydrogen bonding is critical for ketal-containing polyurethane elastomers. Interchain hydrogen-bonding interactions directly affect the morphological structure of polyurethane elastomers. In the ketal-containing polyurethane elastomer, carbamate groups can provide protons, while the carbonyl oxygen in carbamate, oxygen in the ketal, and ether oxygen in PTMG can accept protons. Therefore, hydrogen bonding can form between hard-hard segments or hard-soft segments (Fig. S6a in ESI). The oxygen atom in the soft segment has a relatively lower electron cloud density than that in the hard segment. Thus, the hydrogen-bonding interaction between hard-soft segments was relatively weaker, and its dissociation occurred within the range of 60–80 °C. However, dissociation occurs in the range of 80–120 °C or even higher when hydrogen bonds form between hard-hard segments.[30] Based on the DSC results, it can be inferred that the dominant interchain interaction is hydrogen bonding between hard-soft segments when the soft segment length is relatively short, resulting in a relatively low

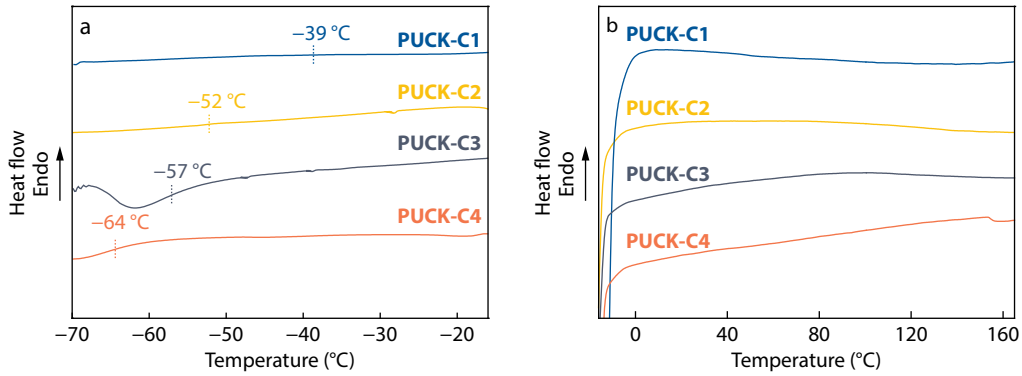

Fig. 3 DSC curves of ketal-containing cross-linking polyurethane elastomers: (a) in the low temperature range and (b) in the high temperature range.

https://doi.org/10.1007/s10118-025-3474-8

degree of phase separation. The hydrogen bonding between hard-hard segments is dominant when the soft segment length is relatively long, leading to a relatively significant phase separation. In other words, the hard segment-rich domains are distributed within the amorphous soft segment phase. Therefore, as the soft segment length increased, the glass transition temperature in the low-temperature region continuously decreased, and the endothermic phenomenon in the high-temperature region shifted towards higher temperatures.

AFM was used to verify this hypothesis. Fig. 4 shows AFM phase images of **PUCK-C*x*** samples. It can be seen that the dark areas represent the hard segment-rich domains and the bright areas represent the soft segment domains. In other words, a phase-separated structure occurred in **PUCK-C*x*** samples. In addition, the size of the hard-segment-rich domain increased gradually as the soft segment length increased. The degree of phase separation showed an increasing trend, which is consistent with the DSC results.

The bands assigned to the urethane C=O stretching vibration in the FTIR spectra were analyzed using multi-peak Gaussian fitting (Fig. S6b in ESI) to further quantify the interchain

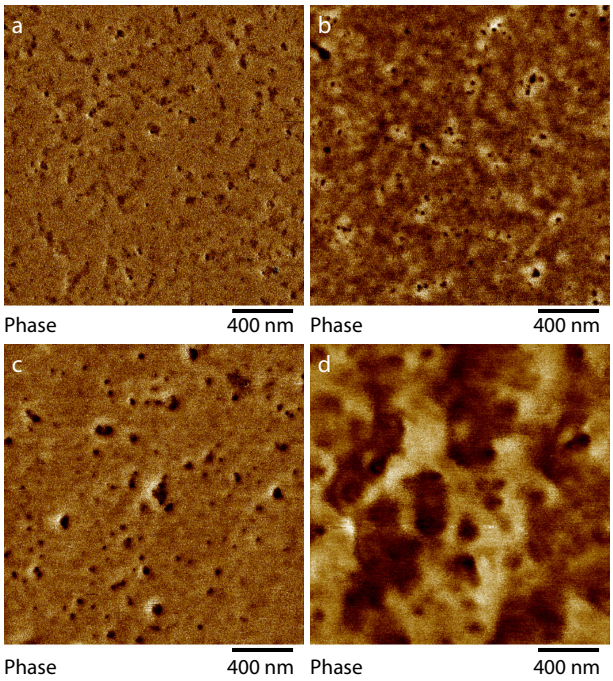

Fig. 4 AFM phase images of ketal-containing cross-linking polyurethane elastomers: (a) **PUCK-C1**, (b) **PUCK-C2**, (c) **PUCK-C3**, and (d) **PUCK-C4**.

hydrogen-bonding interactions. The obtained hydrogen bonding index (X_B) values are listed in Table 2.[31,32] The hydrogen bonding index of the carbonyl showed an increasing trend as the soft segment length increased. The hydrogen bonding of urethane C=O only reflects the hydrogen bonding interaction between hard-hard segments in **PUCK-C*x*** elastomers. Therefore, the increase in the soft segment length promotes the formation of hydrogen bonds between hard-hard segments. In addition to hydrogen bonding with the hard segments, urethane N—H can also form hydrogen bonds with the soft segments. The bands at 3450, 3350, and 3290 cm^{-1} were attributed to the stretching vibrations of free N—H, hydrogen-bonded N—H between hard-soft segments, and hydrogen-bonded N—H between hard-hard segments, respectively.[33,34] The multipeak Gaussian fitting of the bands is presented in Fig. S6(c) (in ESI). The hydrogen bonding proportions of the hard-soft $R_{B(H\text{-}S)}$ and hard-hard $R_{B(H\text{-}H)}$ segments were obtained by calculating the peak areas, as shown in Table 2. It was found that as the soft segment length increased, the hydrogen bonding proportion between hard-soft segments continuously decreased, while the hydrogen bonding proportion between hard-hard segments continuously increased. This is consistent with the inference obtained from the DSC results.

It can be concluded from the above analyses that the interchain interactions mainly originate from the hydrogen bonding between the hard-hard or hard-soft segments. As the soft segment length increased, the hydrogen bonding between hard-hard segments increased gradually, while the hydrogen bonding between hard-soft segments gradually decreased. It can be inferred that the polarization relaxation behavior of polar bonds, such as N—H, C=O, and C—O bonds, can be affected by hydrogen bonding.[35]

Influence of the Soft Segment Length on the Dielectric Properties of Ketal-containing Polyurethane

The dielectric constants and dielectric losses of the **PUCK-C*x*** elastomers are shown in Fig. 5. The electrical conductivity and impedance are shown in Fig. S7 (in ESI). As can be seen, all **PUCK-C*x*** elastomers exhibit relatively high dielectric constants and relatively low dielectric loss factors in the frequency range of 10^3–10^5 Hz. In addition, as the soft segment length increased, the dielectric constant of the elastomer decreased, and the dielectric loss factor also decreased. The electrical conductivity and impedance exhibited a monotonic trend with an increase in the soft segment length.

The *P-E* hysteresis loops of **PUCK-C*x*** elastomers are shown in Fig. S8 (in ESI). The density of the energy storage and the energy storage efficiency obtained are shown in Fig. 6. As can

Table 2 Bands, absorbance ratio, and hydrogen bonding index of carbamate C=O and N—H in FTIR spectra.

Sample	C=O		A_F/A_B [a]	$X_{B(H\text{-}H)}$ [b]	N—H			$R_{B(H\text{-}S)}$	$R_{B(H\text{-}H)}$
	Free	Bonded			Free	$Bonded_{(H\text{-}S)}$	$Bonded_{(H\text{-}H)}$		
PUCK-C1	1730	1708	0.61	0.60	3450	3351	3291	0.58	0.13
PUCK-C2	1730	1709	0.57	0.61	3451	3350	3283	0.50	0.35
PUCK-C3	1732	1710	0.55	0.62	3451	3351	3288	0.46	0.30
PUCK-C4	1732	1711	0.47	0.66	3452	3352	3286	0.44	0.45

[a] A_F and A_B are the absorbances of free and hydrogen-bonded carbamate C=O, respectively; [b] $X_B = (1 + \gamma A_F/A_B)^{-1}$, where X_B is the hydrogen bonding index and γ=1.1 represents the molar extinction coefficient ratio of hydrogen bonded to free carbamate C=O.[31]

https://doi.org/10.1007/s10118-025-3474-8

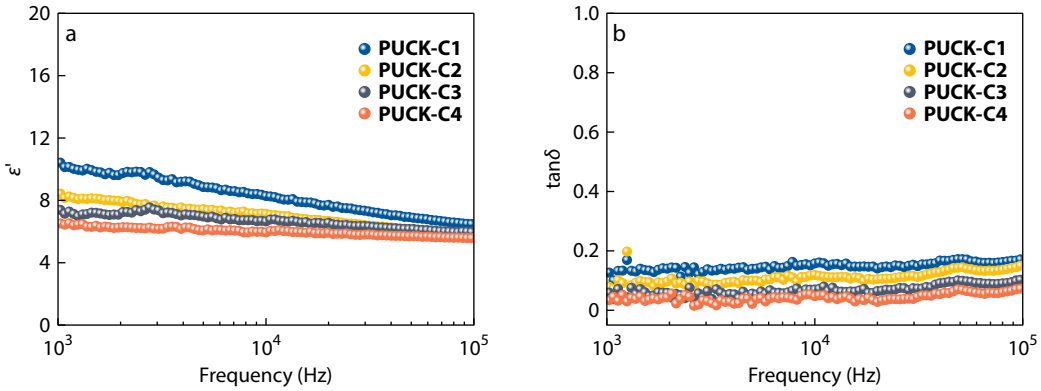

Fig. 5 Dielectric properties of ketal-containing cross-linking polyurethane elastomers: (a) ε' versus frequency curves and (b) tanδ versus frequency curves.

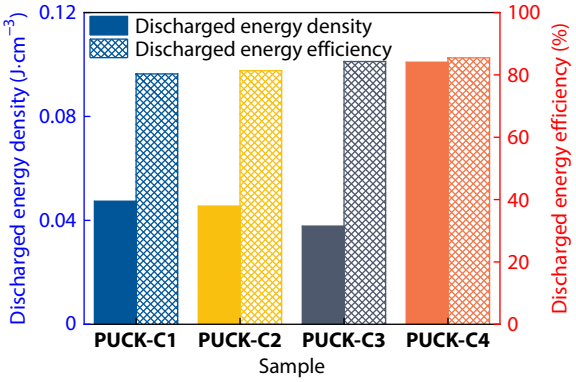

Fig. 6 Discharged energy density and efficiency of ketal-containing cross-linking polyurethane elastomers.

be seen, except for **PUCK-C4**, as the soft segment length increases, the density of energy storage generally shows a decreasing trend, whereas the energy storage efficiency increases gradually.

Ketal-containing cross-linked polyurethane elastomers contain polarizable aromatic rings and polar C=O, C—O and N—H bonds. At the same time, the T_g of soft segments is much lower than room temperature, and no crystalline phase exists in either the soft segment or hard segment phase. Therefore, the polar bonds and aromatic rings can be polarized under the action of an electric field, resulting in relatively high dielectric constants for all elastomers. As the soft segment length increased, the proportion of hydrogen bonding between hard-soft segments in the ketal-containing polyurethane elastomer gradually decreased, while the proportion of hydrogen bonding between hard-hard segments gradually increased. Because the hydrogen bonding between hard-soft segments is a relatively weak interaction, it is relatively easy for the polar bonds to overcome the weak interaction and produce polarization under the action of an electric field. This is the main source of the dielectric constant, and simultaneously causes a relatively large dielectric loss. However, the hydrogen bonding between hard-hard segments is a relatively strong interaction, and it is difficult for the polar bonds to overcome the strong interaction and rotate under the action of an electric field. Thus, the crankshaft motion of ether oxygen-containing segments can appear under the action of an electric field,[36] that is, the secondary source of the dielectric constant, which causes a relatively low dielectric loss. Therefore, as the soft segment length increased, the dielectric constant of the ketal-containing polyurethane elastomer gradually decreased, and the dielectric loss also gradually decreased. The energy storage density is directly related to the dielectric constant and electric field strength. When the electric field strength is constant, the energy storage density depends mainly on the dielectric constant. The energy storage efficiency relies on the dielectric loss. As a result, except for **PUCK-C4**, as the soft segment length increased, the energy storage density of the ketal-containing cross-linked polyurethane elastomer showed a decreasing trend, whereas the energy storage efficiency gradually increased.

The relaxation activation energies obtained from the dielectric relaxation spectra at different temperatures were used to determine the reasons for the changes in the dielectric constant and dielectric loss of **PUCK-C*x*** elastomers. The dielectric relaxation spectra of **PUCK-C*x*** elastomers at different temperatures are shown in Fig. S9 (in ESI). As can be seen, two extreme values of dielectric loss occur in the low- and high-frequency regions. One extreme value appeared between 10^1–10^2 Hz. The relaxation time can be calculated using the equation $\tau = (2\pi f)^{-1}$.[37] If lnτ is plotted against $1/T$, the data points conform to the Arrhenius equation. The relaxation activation energy was obtained using a linear regression relationship, as shown in Fig. 7(a). The relaxation activation energy in the range of 10–20 kJ·mol^{-1} corresponds to the breakage of hydrogen bonds between the hard-soft segments.[38]

The other extreme value of the loss factor appears between 10^4–10^5 Hz. The dielectric relaxation activation energy can be obtained from the slope of the plot of lnτ versus $1/T$, as shown in Fig. 7(b). The activation energy in the range of 0.7–1.7 kJ·mol^{-1} can correspond to the crankshaft motions of ether oxygen-containing segments.[39–41] Therefore, when polarization occurs under the action of an electric field, dielectric loss is relatively low.

Based on the above analyses, the polar bonds in **PUCK-C*x*** elastomer overcome the hydrogen bonding interaction between hard-soft segments to produce polarization under the action of an electric field, and the crankshaft motions of ether oxygen-containing segments in the hard segment-rich re-

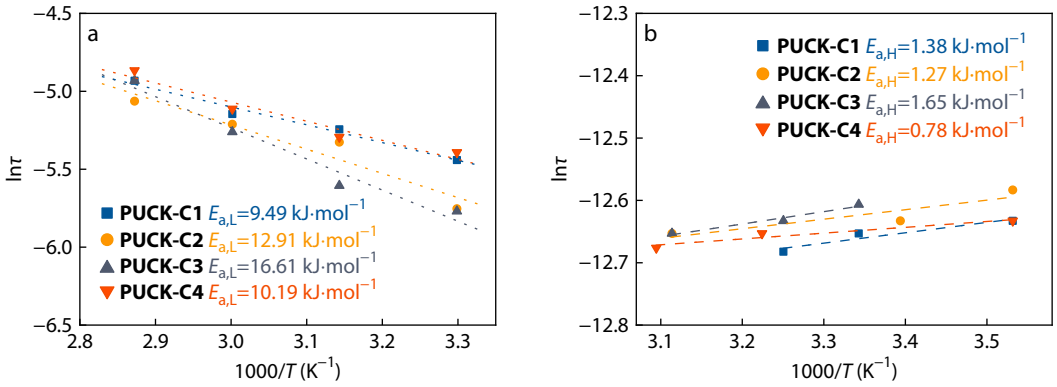

Fig. 7 Activation energy for dielectric relaxation of ketal-containing cross-linking polyurethane elastomers: (a) in the low frequency region and (b) in the high frequency region.

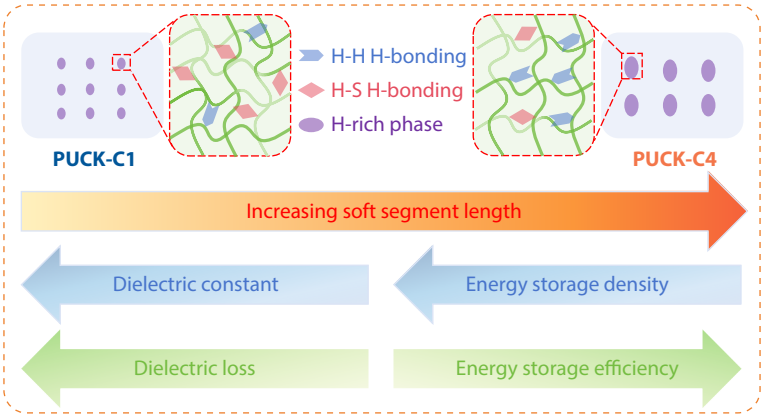

Fig. 8 Influence of soft segment length on the dielectric properties of ketal-containing cross-linking polyurethane elastomers and its cause.

gions also contribute to the polarization. When the soft segment length increased, the proportion of hydrogen bonding between hard-soft segments decreased, while the proportion of hydrogen bonding between hard-hard segments increased. Therefore, the dielectric constant gradually decreased, and the dielectric loss also decreased, as shown in Fig. 8.

CONCLUSIONS

Ketal-containing cross-linked polyurethane elastomers with different soft segment lengths were prepared using cyclic ketal diol as the chain extender and glycerol as the crosslinking agent. Owing to the asymmetry of the cyclic ketal and cross-linked structure, no detectable crystallization occurred in either the hard or soft segment domains of the elastomer. As the soft segment length increases, the proportion of hydrogen bonding between hard-soft segments in the elastomer decreases continuously, while the proportion of hydrogen bonding between hard-hard segments gradually increases. That is, the phase separation becomes increasingly noticeable. Under the action of an electric field, the polar C=O, C—O, and N—H bonds in the ketal-containing polyurethane elastomer, on the one hand, overcome the hydrogen bonding between hard-soft segments to produce polarization; on the other hand, they also experience the crankshaft motions to generate polarization. The former has a relatively high relaxation activation energy of approximately 10–20 kJ·mol^{-1}, resulting in a large dielectric loss. The latter has a relatively low relaxation activation energy, approximately 0.7–1.7 kJ·mol^{-1}, leading to low dielectric loss. Therefore, as the soft segment length increased, the dielectric constant and dielectric loss decreased. This work provides a theoretical foundation for improving the energy storage density and efficiency of polyurethane elastomers.

Conflict of Interests

The authors declare no interest conflict.

Electronic Supplementary Information

Electronic supplementary information (ESI) is available free of charge in the online version of this article at http://doi.org/10.1007/s10118-025-3474-8.

Data Availability Statement

The data supporting the findings of this study are available from the corresponding author upon reasonable request.

ACKNOWLEDGMENTS

This work was financially supported by the Hubei Key

Graphical Abstract

Influence of Soft Segment Length on the Dielectric Polarization Behavior of Ketal-containing Polyurethane Elastomer

Xue Mei, Wan Lu, Jian-Rong Dong, Ke-Heng Pan, Jun-Jie Tan, Hong-Ye Yan, Jun Wu, Yu Zhou, and Hong-Xiang Chen

Wuhan University of Science and Technology; Hubei Normal University

The ketal-containing cross-linked polyurethane elastomers were prepared using cyclic ketal diol as a chain extender. As the soft segment length increases, the hard-soft hydrogen bonding decreases, while the hard-hard hydrogen bonding increases. As a result, the dielectric constant shows a decreasing trend, and the dielectric loss also gradually decreases.

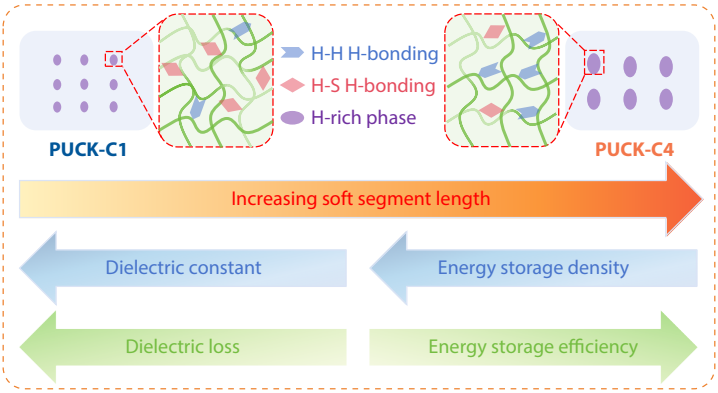

Chinese J. Polym. Sci. 2026, 44, 189–197 *https://doi.org/10.1007/s10118-025-3474-8*

Laboratory of Pollutant Analysis & Reuse Technology (No. PA230102). We would like to thank Wei Yuan at the Analytical & Testing Center of Wuhan University of Science and Technology for his help with AFM analyses.

REFERENCES

1 Feng, Q. K.; Zhong, S. L.; Pei, J. Y.; Zhao, Y.; Zhang, D. L.; Liu, D. F.; Zhang, Y. X.; Dang, Z. M. Recent progress and future prospects on all-organic polymer dielectrics for energy storage capacitors. *Chem. Rev.* **2022**, *122*, 3820–3878.
2 Zhang, Y.; Wang, Y.; He, X.; Hao, G.; Gong, Z.; Zhang, C.; Zhang, Y.; Zhang, T.; Yi, H.; Wang, Q. Tailored sandwich structures in all-organic dielectric composite to optimize energy storage performance. *J. Energy Storage* **2025**, *130*, 117457.
3 Li, W.; Meng, Q.; Zheng, Y.; Zhang, Z.; Xia, W.; Xu, Z. Electric energy storage properties of poly(vinylidene fluoride). *Appl. Phys. Lett.* **2010**, *96*, 192905.
4 Chen, K.; Du, B. X.; Liu, H.; Xiao, M. Enhanced high-temperatures energy storage performance of BOPP film *via* surface grafting modification. *Chem. Eng. J.* **2025**, *505*, 159724.
5 Venkat, N.; Dang, T. D.; Bai, Z.; McNier, V. K.; DeCerbo, J. N.; Tsao, B. H.; Stricker, J. T. High temperature polymer film dielectrics for aerospace power conditioning capacitor applications. *Mater. Sci. Eng. B* **2010**, *168*, 16–21.
6 Ma, R.; Baldwin, A. F.; Wang, C.; Offenbach, I.; Cakmak, M.; Ramprasad, R.; Sotzing, G. A. Rationally designed polyimides for high-energy density capacitor applications. *ACS Appl. Mater. Interfaces* **2014**, *6*, 10445–10451.
7 Xu, W. H.; Tang, Y. D.; Yao, H. Y.; Zhang, Y. H. Dipolar glass polymers for capacitive energy storage at room temperatures and elevated temperatures. *Chinese J. Polym. Sci.* **2022**, *40*, 711–725.
8 Pei, J. Y.; Yin, L. J.; Zhong, S. L.; Dang, Z. M. Suppressing the loss of polymer-based dielectrics for high power energy storage. *Adv. Mater.* **2023**, *35*, 2203623.
9 Zhang, T.; Sun, H.; Yin, C.; Jung, Y. H.; Min, S.; Zhang, Y.; Zhang, C.; Chen, Q.; Lee, K. J.; Chi, Q. Recent progress in polymer dielectric energy storage: from film fabrication and modification to capacitor performance and application. *Prog. Mater. Sci.* **2023**, *140*, 101207.
10 Ma, L.; Zhang, Q.; Cui, C.; Zhong, Q.; Chen, X.; Li, Z.; Mariappan, A.; Cheng, Y.; Zhang, Z.; Zhang, Y. Introduction of a stable radical in polymer capacitor enables high energy storage and pulse discharge efficiency. *Chem. Mater.* **2020**, *32*, 9355–9362.
11 He, Y.; Zhang, G.; Qin, B.; Li, W.; He, G.; Zhu, B.; Zhang, X.; Tan, S.; Zhang, Z. Excellent dielectric energy storage performance achieved by synergistically increasing the permittivity and breakdown strength of poly(vinylidene chloride-*co*-vinyl chloride) with a stabilized conformation. *J. Mater. Chem. A* **2024**, *12*, 21824–21829.
12 Chen, J.; Wang, Z.; Wang, P.; Chen, W.; Wang, Y. Superior electric displacement and energy storage density in dielectric polymer *via* inserting thermoplastic polyurethane. *J. Energy Storage* **2024**, *86*, 111365.
13 Khanchaitit, P.; Han, K.; Gadinski, M. R.; Li, Q.; Wang, Q. Ferroelectric polymer networks with high energy density and improved discharged efficiency for dielectric energy storage. *Nat. Commun.* **2013**, *4*, 3845.

14 Li, Q.; Tan, S.; Gong, H.; Lu, J.; Zhang, W.; Zhang, X.; Zhang, Z. Influence of dipole and intermolecular interaction on the tuning dielectric and energy storage properties of polystyrene-based polymers. *Phys. Chem. Chem. Phys.* **2021**, *23*, 3856–3865.
15 Li, H.; Zhou, Y.; Liu, Y.; Li, L.; Liu, Y.; Wang, Q. Dielectric polymers for high-temperature capacitive energy storage. *Chem. Soc. Rev.* **2021**, *50*, 6369–6400.
16 Shi, M.; Sun, J.; Fang, Q. Alkyl side-chain-induced improvement of dielectric properties of polymers. 1. Fluorene-benzocyclobutene-based polymers. *Macromolecules* **2024**, *57*, 6140–6145.
17 Li, Z.; Wen, Y.; Song, Z.; Zhang, C.; Cui, C.; An, D.; Ge, Z.; Cheng, Y.; Zhang, Q.; Zhang, Y. Dynamic cross-linked polyethylene networks with high energy storage and electrical damage self-healability. *ACS Macro Lett.* **2023**, *12*, 1409–1415.
18 Mao, P.; Wang, J.; Zhang, L.; Sun, Q.; Liu, X.; He, L.; Liu, S.; Zhang, S.; Gong, H. Tunable dielectric polarization and breakdown behavior for high energy storage capability in P(VDF-TrFE-CFE)/PVDF polymer blended composite films. *Phys. Chem. Chem. Phys.* **2020**, *22*, 13143–13153.
19 Delebecq, E.; Pascault, J. P.; Boutevin, B.; Ganachaud, F. On the versatility of urethane/urea bonds: reversibility, blocked isocyanate, and non-isocyanate polyurethane. *Chem. Rev.* **2013**, *113*, 80–118.
20 Lorenzini, R. G.; Kline, W. M.; Wang, C. C.; Ramprasad, R.; Sotzing, G. A. The rational design of polyurea & polyurethane dielectric materials. *Polymer* **2013**, *54*, 3529–3533.
21 Qi, G.; Yang, W.; Puglia, D.; Wang, H.; Xu, P.; Dong, W.; Zheng, T.; Ma, P. Hydrophobic, UV resistant and dielectric polyurethane-nanolignin composites with good reprocessability. *Mater. Des.* **2020**, *196*, 109150.
22 Mannodi-Kanakkithodi, A.; Treich, G. M.; Huan, T. D.; Ma, R.; Tefferi, M.; Cao, Y.; Sotzing, G. A.; Ramprasad, R. Rational co-design of polymer dielectrics for energy storage. *Adv. Mater.* **2016**, *28*, 6277–6291.
23 Dong, J.; Yan, H.; Lv, X.; Wang, Z.; Rao, Z.; Zhu, B.; Wu, J.; Zhou, Y.; Chen, H. Reprocessable polyurethane elastomers based on reversible ketal exchange: dielectric properties and water resistance. *J. Mater. Chem. C* **2023**, *11*, 1369–1380.
24 Yuan, D.; Chen, M.; Xu, Y.; Huang, L.; Ma, J.; Peng, Q.; Cai, X. High-performance PA1/TPU films with enhanced dielectric constant and low loss tangent. *J. Appl. Polym. Sci.* **2020**, *137*, 48469.
25 Zheng, M. S.; Zha, J. W.; Yang, Y.; Han, P.; Hu, C. H.; Wen, Y. Q.; Dang, Z. M. Polyurethane induced high breakdown strength and high energy storage density in polyurethane/poly(vinylidene fluoride) composite films. *Appl. Phys. Lett.* **2017**, *110*, 252902.
26 Le Goupil, F.; Salvado, V.; Rothan, V.; Vidil, T.; Fleury, G.; Cramail, H.; Grau, E. Bio-based poly(hydroxy urethane)s for efficient organic high-power energy storage. *J. Am. Chem. Soc.* **2023**, *145*, 4583–4588.
27 Wu, X.; Chen, X.; Zhang, Q. M.; Tan, D. Q. Advanced dielectric polymers for energy storage. *Energy Storage Mater.* **2022**, *44*, 29–47.
28 Yang, B.; Liu, Y.; Li, W.; Lan, S.; Dou, L.; Zhu, X.; Li, Q.; Nan, C. W.; Lin, Y. H. Balancing polarization and breakdown for high capacitive energy storage by microstructure design. *Adv. Mater.* **2024**, *36*, 2403400.
29 He, Q.; Sun, K.; Shi, Z.; Liu, Y.; Fan, R. Polymer dielectrics for capacitive energy storage: from theories, materials to industrial capacitors. *Mater. Today* **2023**, *68*, 298–333.
30 Wang, W.; Chen, H.; Dai, Q.; Zhao, D.; Zhou, Y.; Wang, L.; Zeng, D. Thermally healable PTMG-based polyurethane elastomer with robust mechanical properties and high healing efficiency. *Smart Mater.* Struct. **2019**, *28*, 015008.
31 Senich, G. A.; MacKnight, W. J. Fourier transform infrared thermal analysis of a segmented polyurethane. *Macromolecules* **1980**, *13*, 106–110.
32 Niu, Z.; Wang, Y.; Wang, X.; Yin, D.; Shou, T.; Cao, P.; Zhao, X.; Hu, S.; Zhang, L. Investigating the effect of chain extender on the phase separation and mechanical properties of polybutadiene-based polyurethane. *Macromol. Rapid Commun.* **2024**, *45*, 2400259.
33 Zhang, C.; Hu, J.; Li, X.; Wu, Y.; Han, J. Hydrogen-bonding interactions in hard segments of shape memory polyurethane: toluene diisocyanates and 1,6-hexamethylene diisocyanate. a theoretical and comparative study. *J. Phys. Chem. A* **2014**, *118*, 12241–12255.
34 Sun, H. Ab initio characterizations of molecular structures, conformation energies, and hydrogen-bonding properties for polyurethane hard segments. *Macromolecules* **1993**, *26*, 5924–5936.
35 Jiang, X.; Xu, M.; Wang, M.; Ma, Y.; Zhang, W.; Zhang, Y.; Rong, H.; Lu, X. Preparation and molecular dynamics study of polyurethane damping elastomer containing dynamic disulfide bond and multiple hydrogen bond. *Eur. Polym. J.* **2022**, *162*, 110893.
36 Helfand, E.; Wasserman, Z. R.; Weber, T. A. Brownian dynamics study of polymer conformational transitions. *Macromolecules* **1980**, *13*, 526–533.
37 Guerrero-Ruiz, F.; Bonardd, S.; Otaegi, I.; Verde-Sesto, E.; Maiz, J. Probing the remarkable vitrimeric performance of poly (dithiourethanes): a comprehensive investigation into the dynamic behavior. *Eur. Polym. J.* **2024**, *217*, 113305.
38 Ren, Z.; Ma, D.; Yang, X. H-bond and conformations of donors and acceptors in model polyether based polyurethanes. *Polymer* **2003**, *44*, 6419–6425.
39 Castagna, A. M.; Fragiadakis, D.; Lee, H.; Choi, T.; Runt, J. The role of hard segment content on the molecular dynamics of poly(tetramethylene oxide)-based polyurethane copolymers. *Macromolecules* **2011**, *44*, 7831–7836.
40 Fragiadakis, D.; Runt, J. Molecular dynamics of segmented polyurethane copolymers: influence of soft segment composition. *Macromolecules* **2013**, *46*, 4184-4190.
41 Kanapitsas, A.; Pissis, P. Dielectric relaxation spectroscopy in crosslinked polyurethanes based on polymer polyols. *Eur. Polym. J.* **2000**, *36*, 1241–1250.

https://doi.org/10.1007/s10118-025-3474-8